Microelectronics Reliability 50 (2010) 959–964

Contents lists available at ScienceDirect

Microelectronics Reliability

journal homepage: www.elsevier.com/locate/microrel

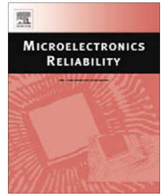

Failure and degradation mechanisms of high-power white light emitting diodes

Shih-Chun Yang [a], Pang Lin [a], Chien-Ping Wang [b,*], Sheng Bang Huang [b], Chiu-Ling Chen [b], Pei-Fang Chiang [b], An-Tse Lee [b], Mu-Tao Chu [b]

[a] *Department of Materials Science and Engineering, National Chiao-Tung University, Hsinchu, Taiwan*
[b] *Electronics and Optoelectronics Research Laboratories, ITRI, Chutung, Hsinchi, Taiwan*

A R T I C L E I N F O

Article history:
Received 18 October 2008
Received in revised form 11 March 2010
Available online 3 April 2010

A B S T R A C T

The investigation explores the factors that influence the long-term performance of high-power 1 W white light emitting diodes (LEDs). LEDs underwent an aging test in which they were exposed to various temperatures and electrical currents, to identify both their degradation mechanisms and the limitations of the LED chip and package materials. The degradation rates of luminous flux increased with electrical and thermal stresses. High electric stress induced surface and bulk defects in the LED chip during short-term aging, which rapidly increased the leakage current. Yellowing and cracking of the encapsulating lens were also important in package degradation at 0.7 A/85 °C and 0.7 A/55 °C. This degradation reduced the light extraction efficiency to an extent that is strongly related to junction temperature and the period of aging. Junction temperatures were measured at various stresses to determine the thermal contribution and the degradation mechanisms. The results provided a complete understanding of the degradation mechanisms of both chip and package, which is useful in designing highly reliable and long-lifetime LEDs.

Crown Copyright © 2010 Published by Elsevier Ltd. All rights reserved.

1. Introduction

High-brightness white light emitting diodes (LEDs) have attracted considerable interest in recent years owing to their diverse range of illumination applications, which range including outdoor lights and automobile headlamps. The degradation of stability and luminescence of LEDs has been investigated using long-term aging or operating stress methods. Experiments have been performed using accelerated currents to study power output changes and calculate the half-life [1–3].

Advances in the reliability of high-brightness LEDs have also stimulated considerable interest in extending their lifetimes. The performance of GaN-based LEDs has been examined by exposing them to various DC and pulsed bias conditions [4–7]. Both phosphor degradation and the generation of chip defects can be inferred from variations in the power spectrum and changes in the voltage–capacitance characteristics. The optimal design of electrodes and the transparent layer ensures uniform spreading of current and maximal light efficiency [8]. The accelerated failure mode also indicates that magnesium dopant can reduce quantum well efficiency and increase series resistance, forward voltage, and current crowding [9]. Encapsulating epoxy was tested in a high-temperature aging environment and at the high junction temperature to examine the failure mechanisms of high-power LEDs [10,11].

Although numerous studies have focused on improving the reliability of high-power LEDs, the mechanisms of degradation and the limitations of LED chips and packages are not well understood. In this investigation, high-power white light LEDs (1 W) were aged using various electrical currents and temperatures, to distinguish various degradation mechanisms. Experimental results demonstrate that the luminous efficiency of LEDs is significantly reduced under various aging stresses. The limitations of blue LED chips and encapsulated materials were explored. Thermal, electrical and optical characteristics were analyzed to identify failure mechanisms in both the LED chips and packages.

2. Experiments

As shown in Fig. 1, the treated devices were commercially available 1 W high-power gallium nitride-based white LEDs, whose light extraction was enhanced by a flip chip configuration on a silicon sub-mount. The deposited YAG:Ce yellow phosphor layer above the $1 \times 1\ mm^2$ blue LED chip converted emitted blue light to white light. Plastic lenses were applied to protect the device against atmospheric impurities and to obtain the designed distribution of light from the LED. The gap between the blue LED chip and the lens was filled with a silicone encapsulent. A metal heat sink and an aluminum plate were used to establish the primary thermal path and thus reduce the thermal effect.

Fifty samples were aged under five conditions – 1 A/85 °C, 1 A/55 °C, 0.7 A/85 °C, 0.7 A/55 °C and 0.35 A/25 °C. The treated devices

* Corresponding author.
E-mail address: cpwang@itri.org.tw (C.-P. Wang).

0026-2714/$ - see front matter Crown Copyright © 2010 Published by Elsevier Ltd. All rights reserved.
doi:10.1016/j.microrel.2010.03.007

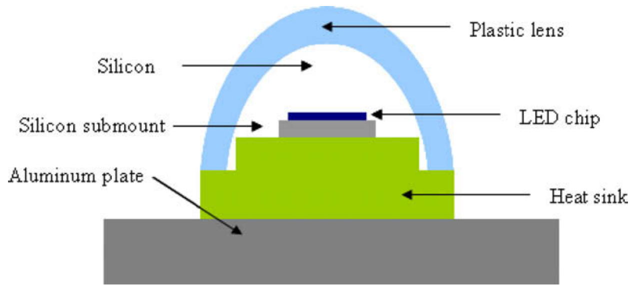

Fig. 1. Schematic diagram of LED structure.

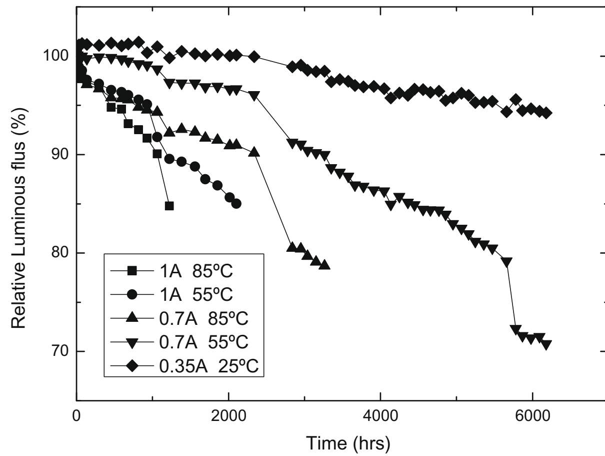

Fig. 2. Relative luminous flux as a function of aging time under the various currents and temperatures.

were placed in a large oven that was maintained at a constant temperature. To elucidate the mechanism of accelerated degradation,

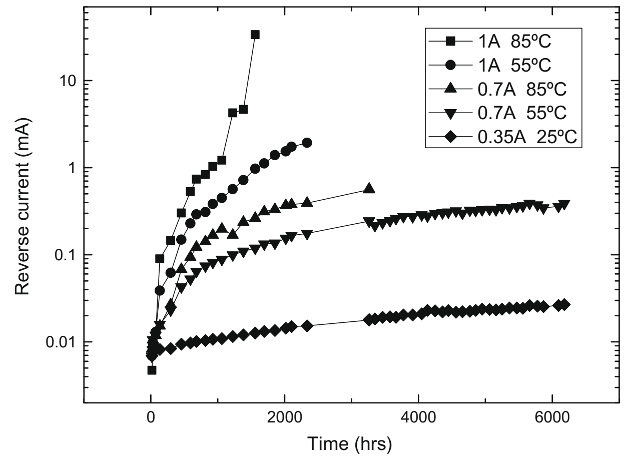

Fig. 3. Reverse current as a function of time under various aging conditions.

700 mA and 1000 mA were applied, which currents exceeded the recommended driving current of 350 mA. Currents of 350 mA, 700 mA and 1 A were applied to a 1×1 mm^2 chip, yielding current densities of 3.5×10^4 mA/cm^2, 7.0×10^4 mA/cm^2 and 1.0×10^5 mA/cm^2, respectively. More than 6000 h of aging tests were performed to identify the long-term degradation under these five operating conditions. The luminous flux, the electroluminescence (EL) spectrum, the current–voltage characteristics, and the transmittance of the epoxy resin lens were investigated to elucidate mechanisms of degradation of the chip or package.

3. Results and discussion

As displayed in Fig. 2, various accelerating aging stresses induced various degradation rates of light output. The luminous fluxes of the 10 treated devices were measured under the same

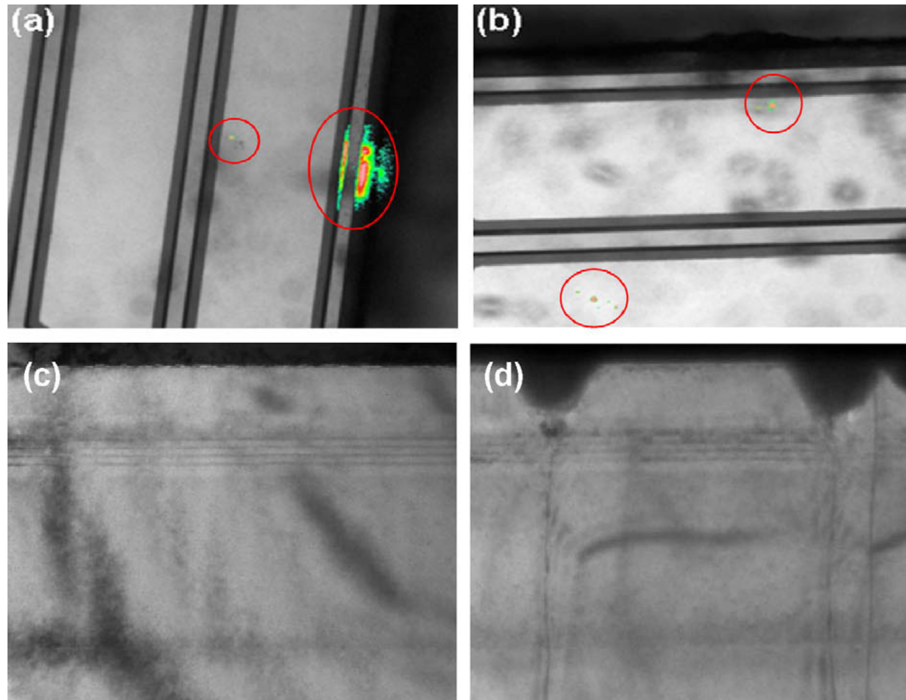

Fig. 4. Top view EMMI images and TEM cross-section images: (a) EMMI image of a treated device at 0.7 A/85 °C after 3264 h, (b) EMMI image of a treated device at 0.7 A/55 °C after 6180 h, (c) TEM image of a normal area after the stress of 0.7 A/55 °C, and (d) TEM image of a hot spot after the stress of 0.7 A/55 °C.

condition, averaged, and normalized to the initial value of the original devices. Thermal degradation was investigated over a range of aging temperatures from 55 °C to 85 °C under a fixed electrical stress. The electrical effect was also studied under various currents from 0.7 A to 1 A at a constant temperature. Under stresses of 1 A/85 °C and 1 A/55 °C, the luminous flux declined rapidly for 1384 and 2104 h, respectively, finally causing early complete failure. Under the normal aging condition, 0.35 A/25 °C, the luminous flux had degraded by only 6% after 6180 h. This stress did not induce the changes of plastic lenses or polymer materials.

To meet commercial specifications, the electrical characteristics of LEDs were measured at a reverse bias of −5 V and a constant temperature of 25 °C. Fig. 3 plots the reverse current as a function of time for various temperatures and currents on a semi-logarithmic scale. Under the conditions 1 A/85 °C and 1 A/55 °C, the reverse current increased substantially in a few hundred hours. After more than 1000 h of aging, the reverse current under the greater electrical stress was more than three orders of magnitude higher than that under normal aging stress. Finally, devices aged

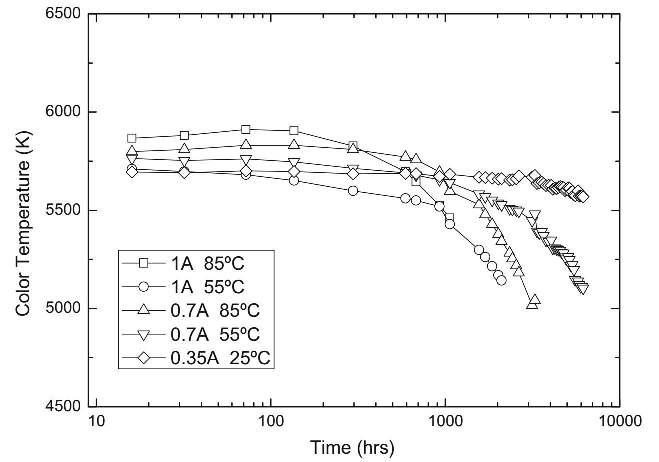

Fig. 6. Color temperature as a function of time under various aging conditions.

Fig. 5. Spectrum distribution before and after various aging tests: (a) stressing current of 0.7 A, oven temperature 85 °C, (b) stressing current of 0.7 A, oven temperature 55 °C, and (c) stressing current of 0.35 A, oven temperature 25 °C.

at 1 A/85 °C failed after 1384 h and exhibited no diode characteristic except for resistive behavior. Devices treated at other aging stresses exhibited similarly increased reverse current. The leakage current increased with the aging stress, which process was accompanied by a decline in radiative efficiency. Restated, the increase in reverse leakage current accompanied the optical degradation. The leakage current could be regarded as tunneling current in a multi-quantum well (MQW) along a conduction path parallel to the *p*–*n* active layer, due to defect generation.

Fig. 4a and b presents the EMMI (emission microscopy) images of leakage current at a reverse bias of −5 V. Infrared emission can occur and be detected in a semiconductor device when excessive electron–hole pair recombination occurs. The infrared detection tool EMMI can be used to detect accurately the sites and number of failures. The hot spots in Fig. 4a and b indicates the leakage locations and the impact area after the aging stress. The leakage current at 0.7 A/85 °C exceeded that at 0.7 A/55 °C. A similar trend in the leakage current was also observed at 1 A/85 °C and 1 A/

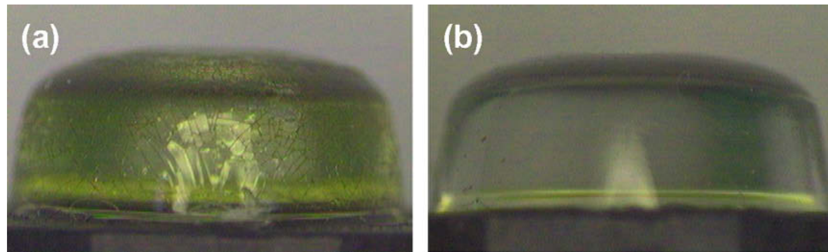

Fig. 7. Optical microscopy images under various aging conditions: (a) stressing current of 0.7 A, oven temperature 85 °C and (b) stressing current of 0.35 A, oven temperature 25 °C.

Fig. 8. Two-dimensional distribution curve of luminous intensity under various aging tests: (a) stressing current of 0.7 A, oven temperature 85 °C, after 3264 h, (b) stressing current of 0.7 A, oven temperature 55 °C, after 6180 h, (c) stressing current of 0.35 A, oven temperature 25 °C, after 6180 h, and (d) original sample.

55 °C. No leakage hot spot was observed in the original samples before aging stress was applied. The generation of defects in the chips increased the reverse-bias current and these defects were strongly related to the threading dislocations of mixed or pure screw character [12]. Fig. 4c and d displays TEM images of a treated device under the stress of 0.7 A/55 °C after 6180 h of aging. As shown in Fig. 4c, there is no obvious defect in the normal area of a treated device. By contrast, Fig. 4d reveals that threading dislocations of the hot spot stem from the V-shaped defects. The corresponding leakage paths caused the large leakage current and significantly reduced the luminous efficiency of LEDs. The EMMI images and TEM cross-section images seem to suggest an increase in the number of leakage paths. Cross-sectional TEM (transmission electron microscopy) micrographs of the LED samples demonstrated that the densities of threading dislocations were around $1.25 \times 10^{10}\ \text{cm}^{-2}$ and $4 \times 10^{10}\ \text{cm}^{-2}$ before and after the aging test, respectively. Consequently, one of the failure mechanisms could be the gradually increased leakage paths [13,14].

Fig. 5 presents the emission spectrum before and after the aging test. It includes 440 nm emission peaks from the LED chip and 556 nm emission peaks from the excited phosphor. The red-shift of the peak wavelength was minor, approximately 2 nm, under the various stresses. At 0.7 A/55 °C, the intensities of the emitted blue and yellow light decayed by almost 49% and 23%, respectively, during a long period of aging. The corresponding values at 0.35 A/25 °C were only 10% and 6%. Subjected to higher electrical and thermal stresses, the intensity of the blue emission declined more rapidly than that of the yellow. The different degradation rate induced the color shift issue and reduced the color temperature. Fig. 6 plots color temperature shifts as a function of aging time. Color temperature is a characteristic of visible light, and was determined herein by comparing its chromaticity with that of an ideal black-body radiator. An object placed in the sun has a different color temperature from the same object under a fluorescent lamp, because each light source has its own specific color temperature. The results reveal that the color temperature decreased by 2% and 10% at 0.35 A/25 °C and 0.7 A/55 °C, respectively, after more than 6000 h of aging tests. At 1 A/85 °C and 0.7 A/85 °C, the color temperature declined by 15% and 7% after 1224 and 3264 h of aging, respectively. Devices were treated under stresses of 1 A/85 °C and 1 A/55 °C to terminate the experiment after the luminous flux had been degraded by approximately 15% because complete failure had by then occurred. The optical micrographic images indicate no obvious package degradation in the encapsulating lenses, implying an absence of package failure under these two aging stresses. Thus, if only comparing these two stresses, failure phenomena suggest that the dominant mechanism of degradation of color temperature could be related to the LED chip due to the reverse leakage current drastically increased. An extremely high current density at the junction interface damaged LED chips and rendered them inactive. In contrast, the encapsulating lenses exhibited obvious yellowing and cracking under both 0.7 A/85 °C and 0.7 A/55 °C conditions in the aging tests. As shown in Fig. 7a, the encapsulated material exhibited apparent lens yellowing and cracking under the stress at 0.7 A/85 °C. No obvious change occurred at 0.35 A/25 °C, as displayed in Fig. 7b. Under the stresses of 0.7 A/55 °C and 0.7 A/85 °C, the degradation mechanisms both involved encapsulated materials and the LED chip, as revealed by the yellowing of the lenses and the simultaneous increase in leakage current. The failure of the encapsulated material is attributable to the applied stress, which influenced the chemical bonding of the encapsulating lenses, causing the sensitivity in thermal stability and photo-degradation after long-term burn-in experiment [15]. This effect is one of the degradation modes that are induced by a high junction temperature and a long aging time, which effectively reduce the light extraction efficiency.

Fig. 8 plots the two-dimensional distribution curve of luminous intensity in various aging tests. After 3264 h of aging at 0.7 A/85 °C, the intensity distribution curve was clearly lower than before, with an irregular symmetric distribution caused by lens yellowing and cracking. The increase in reverse leakage current also reduced the radiative recombination efficiency, causing an overall decline in the intensity distribution. Similar results were obtained under 0.7 A/55 °C after 6180 h of aging. Under 0.35 A/25 °C, after more than 6000 h of aging, no obvious deterioration of the intensity distribution curve was observed. Based on the experimental results, lens yellowing was strongly correlated with both junction temperature and aging time.

Fig. 9 plots the distribution of junction temperature under various aging conditions. The diode forward voltage method was employed to measure the LED junction temperature [16]. The TSP (temperature-sensitive parameter) was measured to establish a correlation between forward voltage and temperature:

$$\text{TSP} = \frac{\Delta V_f}{\Delta T} \tag{1}$$

where V_f is the forward voltage, and T is the oven temperature. A linear fit of Eq. (1) can be written as,

$$V_f = a + bT \tag{2}$$

$$T_j = \frac{V_f - a}{b} \tag{3}$$

Therefore, junction temperature is calculated from the applied driving current. The junction temperatures plotted in Fig. 9 were associated with the different stresses. As the driving current or oven temperature increased, the junction temperature increased dramatically, and was apparently related to the LED lifetime. Non-radiative recombination induced the generation of heat and increased the junction temperature of the devices. An increase in junction temperature may have changed the encapsulated material from transparent to yellow [17,18]. The electrical characteristics and EMMI images revealed degradations at various junction temperatures. The largest difference in junction temperatures was 110 °C between that under the highest stress (1 A/85 °C) and that under the normal condition (0.35 A/35 °C). However, it was noting that the devices under the stresses of 0.7 A/85 °C and 1 A/55 °C showed the approximate junction temperature, but they exhibited the different failure mode. Under the stress of 0.7 A/85 °C, samples exhibited two failure mechanisms – chip degradation and package damage. In the initial aging period, samples exhibited only an increase in leakage current without damage to the lenses, which be-

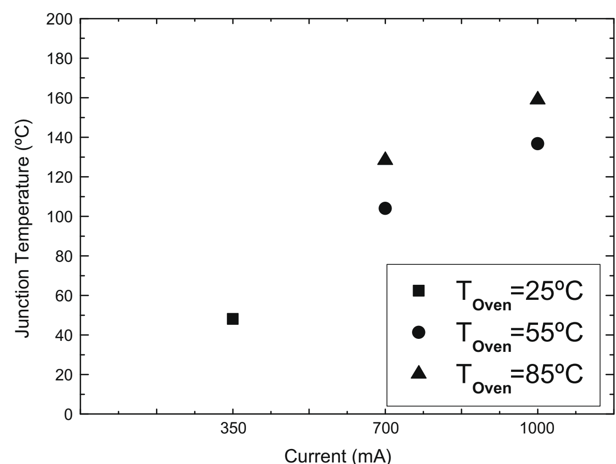

Fig. 9. The distribution of junction temperatures with various currents and oven temperatures.

came yellow after 2000 h. In contrast, under the stress of 1 A/55 °C, the electrical stress induced by the higher forward current was the major cause of the complete failure of the LED chip. Accordingly, we believe that junction temperature was not the only index of burn-in stresses.

4. Conclusion

High-power white light LEDs were aged under various electrical and thermal stresses to analyze their failure and degradation mechanisms. Results provided the sufficient information to elucidate most of the failure mechanisms of high-power LEDs. The large increase in leakage current and the number of EMMI hot spot regions were adopted to demonstrate LED chip degradation, which was caused by the generation of defects in the LED. TEM cross-section images of a hot spot also seem to provide evidence for an increased density of threading dislocations. As the transmittance and the refractive index of the encapsulated materials changed, the light extraction efficiency decreased. This effect was also demonstrated by both optical microscopy and the two-dimensional distribution curve of luminous intensity. Under the conditions 1 A/85 °C and 1 A/55 °C, extremely high electrical stress caused LED chip failure after the short-term aging process. Under the conditions 0.7 A/85 °C and 0.7 A/55 °C, an increase in reverse leakage current and lens yellowing were both observed, which effects were apparently caused by higher junction temperatures and longer aging times. Besides, under the stresses of 1 A/55 °C and 0.7 A/85 °C, treated device with the approximate junction temperature exhibited the different failure mode. Thus, the electrical stress and the thermal stress have an effect in the failure mechanisms, respectively. The results provide a complete analysis of the failure mechanisms of high-power LEDs, and are helpful in designing a high-reliability and high-endurance LEDs.

References

[1] Chen ZZ, Zhao J, Qin ZX, Hu XD, Yu TJ, Tong YZ, et al. Study on the stability of the high-brightness white LED. Phys Stat Sol (B) 2004;241:2664–7.

[2] Pursiainen O, Linder N, Jaeger A, Oberschmid R, Streubel K. Identification of aging mechanisms in the optical and electrical characteristics of light-emitting diodes. Appl Phys Lett 2001;79:2895–7.

[3] Yanagisawa T, Kojima T. Long-term accelerated current operation of white light-emitting diodes. J Lumin 2005;114:39–42.

[4] Barton Daniel L, Osinski Marek. Life tests and failure mechanisms of GaN/AlGaN/InGaN light emitting diodes. Proc SPIE 1998;3279:17–27.

[5] Narendran N, Gu Y, Freyssinier JP, Yu H, Deng L. Solid-state lighting: failure analysis of white LEDs. J Cryst Growth 2004;268:449–56.

[6] Levada S, Meneghini M, Zanoni E, Buso S, Spiazzi G, Meneghesso G. High brightness INGAN LEDs degradation at high injection current bias. In: IEEE 44th annual international reliability physics symposium; 2006. p. 615–6.

[7] Meneghini M, Podda S, Morelli A, Pintus R, Trevisanello L, Meneghesso G, et al. High brightness GaN LEDs degradation during dc and pulsed stress. Microelectron Reliab 2006;46:1720–4.

[8] Xiao Z, He X, Ma K, Chen X, Wu S, Ke Z. The effect of processes on the reliability of GaN based lighting emitting diodes. In: Proc SPIE 6355. p. 63550K-1–9.

[9] Meneghesso G, Levada S, Zanoni E. Failure mechanism of GaN-Based LEDs related with instabilities in doping profile and deep levels. In: IEEE 42nd IRPS; 2004. p. 474–8.

[10] Hsu YC, Lin YK, Chen MH, Tsai CC, Kuang JH, Huang SB, et al. Failure mechanisms associated with lens shape of high-power LED modules in aging test. IEEE Trans Electron Dev 2008;55:689–94.

[11] Xi Y, Gessmann T, XI J, Kim JK, Shah JM, Schubert EF, et al. Junction temperature in ultraviolet light-emitting diodes. Jpn J Appl Phys 2005;44:7260–6.

[12] Cao XA, LeBoeuf SF, D'Evelyn MP, Arthur SD, Kretchmer J, Yan CH, Yang ZH. Blue and near-ultraviolet light-emitting diodes on free-standing GaN substrates. Appl Phys Lett 2004;84:4313–5.

[13] Cao XA, Teetsov JA, Shahedipour-Sandvik F, Arthur SD. Microstructural origin of leakage current in GaN/InGaN light-emitting diodes. J Cryst Growth 2004;264:172–7.

[14] Tomiya S, Hino T, Goto S, Takeya M, Ikeda M. Dislocation related issues in the degradation of GaN-Based laser diodes. J Sel Top Quantum Electron 2004;10(6):1277–85.

[15] Huang JC, Deanin RD, Chu YP, Wei M. Comparison of epoxy resins for applications in light-emitting diodes. Adv Polym Technol 2004;23(4):298–306.

[16] Xi Y, Schubert EF. Junction–temperature measurement in GaN ultraviolet light-emitting diodes using diode forward voltage method. Appl Phys Lett 2004;85:2613–4315.

[17] Senawiratne J, Zhao W, Detchprohm T, Chatterjee A, Li Y, Zhu M, et al. Junction temperature analysis in green light emitting diode dies on sapphire and GaN substrates. Phys Stat Sol (c) 2008;5:2247–9.

[18] Tsai PC, Chuang Ricky W, Su YK. Lifetime tests and junction–temperature measurement of InGaN light-emitting diodes using patterned sapphire substrates. J Lightwave Technol 2007;25:591–6.